

# Loading rate effects during indentation and impact on glass with small spheres

J. PERSSON, K. BREDER\*, D. J. ROWCLIFFE

Royal Institute of Technology, Department of Materials Science and Engineering, S-100 44 Stockholm, Sweden

In order to study the relationship between static and dynamic behaviour of soda–lime glass, both quasi-static and dynamic experiments have been conducted. The difference in material behaviour when using the two test methods suggests a loading-rate dependence in the fracture of glass. To investigate this further, quasi-static tests using different loading rates were made. This investigation showed a clear difference in material behaviour when the loading rate was increased from  $\leq 10 \text{ N s}^{-1}$  to  $\geq 100 \text{ N s}^{-1}$ . The results also suggest that Hertzian theory can be used to calculate contact zone sizes even when simple cracking occurs in quasi-static and dynamic cases. The Hertzian description breaks down once crushing occurs.

## 1. Introduction

Over 100 years ago, Hertz described the static contact between two solids. Since then this problem has been extensively studied [1–6] both theoretically and experimentally and attempts have been made to extend the original theory to dynamic loading. Expressions for the maximum dynamic load delivered to a target have been derived, assuming that all the kinetic energy of the impacting sphere is transformed into strain energy in the target [7, 8].

When the load on the indented material is sufficiently high, the tensile stresses will create a ring crack around the contact zone. According to Hertz theory, this ring crack should be formed at the edge of the contact zone, where the tensile stress has its maximum. Later work [2, 9] has shown that this is not always the case. Often the ring crack is formed outside the contact zone. Attempts to explain this include discussion of the role played by the friction between the two different materials [2] and the statistical distribution of surface flaws [9]. The ring crack can develop further to create a cone crack. This configuration is sometimes called a Hertzian fracture. Cook and Pharr have given a review of the different crack systems formed during indentation with sharp indentors [10]. Most of these crack systems (cone, radial, median, half-penny and lateral cracks) can also be seen when indentations are made with a spherical indenter at sufficiently high loads. The different indentation techniques that can be used have been described by Rowcliffe [11] (indenter shapes, load ranges, stress fields). If the indentations with a spherical indenter are kept within the limits required by Hertz theory, some material parameters can be determined, for example fracture toughness [1, 12] and elastic modulus [13].

Another aspect of quasi-static indentation that has not been studied before is the loading-rate dependence. If the loading rate is high enough, the indenta-

tion should be called impact and there must exist some transition between the two cases. Impact damage on glass and other brittle materials has been studied before [7–9, 14–19] but with few comparisons with quasi-static indentations. In this work, similarities and differences between quasi-static indentation- and impact-induced damage are reported and discussed.

## 2. Experimental procedure

Both dynamic and quasi-static experiments have been performed during the experimental work. The projectiles and indentors were identical steel spheres (SKF AB, Sweden;  $E \approx 200 \text{ GPa}$ ,  $\nu \approx 0.3$ ,  $\rho \approx 7800 \text{ kg m}^{-3}$ ), 3 mm in diameter. For some of the impacts 3 mm diameter cobalt bonded WC spheres (Spheric Engineering Ltd, UK;  $E \approx 614 \text{ GPa}$ ,  $\nu \approx 0.22$ ,  $\rho \approx 14100 \text{ kg m}^{-3}$ ) were used. The target material was soda–lime glass ( $E \approx 70 \text{ GPa}$ ,  $\nu \approx 0.25$ ). All glass pieces were cut from a large plate and were approximately  $50 \text{ mm} \times 50 \text{ mm} \times 15 \text{ mm}$ . The indentations and impacts were made on one of the large faces.

The impacts were made using a small gas gun. It has a 570 mm long barrel with inner diameter 3 mm and is loaded with compressed nitrogen. The gas is released by puncturing a thin (0.025 or 0.050 mm) brass diaphragm with a spring-loaded needle. The velocity of the projectile was measured with a commercially available system (Weinlich GmbH and Co, Reilingen, Germany) designed to measure the projectile velocity of various air guns. This system works by the principle of time-of-flight between two lightbeams 25 cm apart. The measured velocities were in the range  $20\text{--}225 \text{ m s}^{-1}$ .

A computer-controlled universal testing machine (Instron, High Wycombe, UK), where the loading rate and maximum load can be carefully controlled, was used for the quasi-static indentations. The tests were

\* Present address: Oak Ridge National Laboratory, Metals and Ceramics Division, Tennessee, USA

run in load control mode. The load was raised to the fixed value (in the range 100–4500 N) at the selected loading rate (0.05, 5, 10, 100, 200 or 500 N s<sup>-1</sup>). When the maximum load was reached, the unloading began immediately with the same unloading rate as loading rate. The reason for not holding the specimen at the maximum load for any time was to simulate the loading cycle at an impact, although at a very much lower loading rate.

After a completed test, the indented or impacted sample was examined in an optical microscope equipped with a video measurement device that made it possible to measure accurately the size of the contact zone and various cracks. In some tests, the true contact zone was measured by applying a thin layer of Au–Pd to the glass with an ordinary sputter-coater before indentation or impacting [13].

### 3. Results

The measurements made in these experiments are the radius of the contact zone on coated samples, the radius of ring cracks, the size of cone cracks, and the length of radial and lateral cracks. Crushing occurred under the most severe quasi-static and impacting conditions. It was difficult to define a clear boundary between crushing and cracking, see Fig. 1, and therefore the size of the crushed area is subject to some uncertainty.

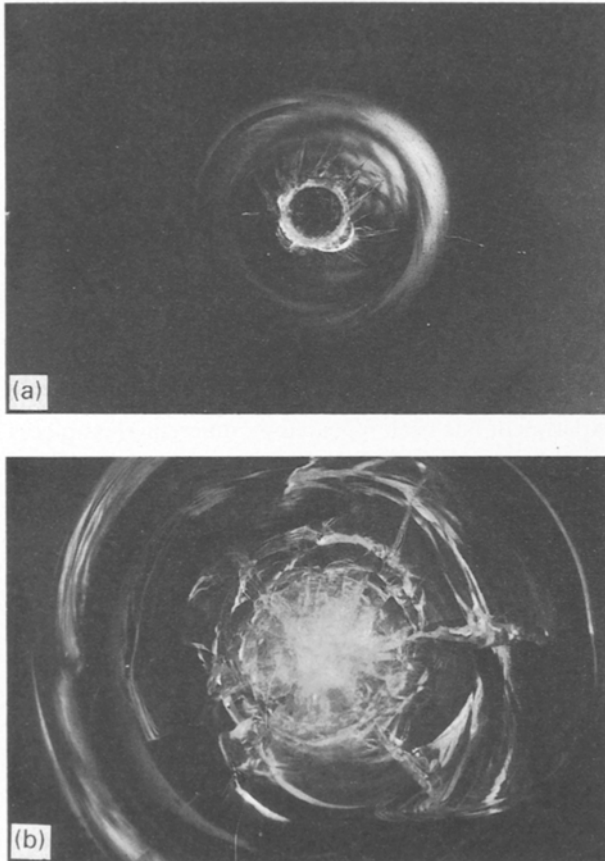


Figure 1 Impact on glass with a 3 mm diameter hardened steel sphere. The magnification is the same in both photos. (a) Velocity  $v = 40.9 \text{ m s}^{-1}$ . Radius of the largest ring crack,  $r = 400 \text{ } \mu\text{m}$ . (b) velocity  $v = 48.1 \text{ m s}^{-1}$ . It is difficult to define a boundary between crushing and cracking.

TABLE I The radius of the largest ring crack appearing after quasi-static indentation with steel spheres at different maximum loads at four different loading rates

Load (N)	Radius ( $\mu\text{m}$ )			
	5 N s <sup>-1</sup>	10 N s <sup>-1</sup>	100 N s <sup>-1</sup>	500 N s <sup>-1</sup>
100	—	—	—	—
200	198	202	—	—
300	282	224	—	—
400	255	244	—	—
500	258	259	242	249
600	280	276	278	280
700	298	302	370	—
800	311	328	315	—
900	328	323	315	330
1000	345	357	384	352
1100	364	398	396	370
1200	386	364	374	365
1300	379	390	375	382
1400	392	375	472	403
1500	415	416	378	423
1600	414	409	394	415
1700	428	412	389	420
1800	440	438	435	430

TABLE II The radius of the largest ring crack appearing after impacting with steel spheres at different velocities

Velocity ( $\text{m s}^{-1}$ )	Radius ( $\mu\text{m}$ )
30.9	359
37.4	395
39.6	458
39.6	290
39.9	455
40.1	450
40.1	425
40.9	400
44.6	430

On all quasi-static indentations and the impacts at low velocities, where no crushing occurs, the radius of the largest ring crack was measured, Table I (quasi-static) and Table II (impact). Because the testing machine gives slightly different maximum loads for different runs, the load in Table I is rounded off to the nearest multiple of 100 N, but is never more than  $\pm 10 \text{ N}$  from this figure (in most cases the measured load is 0–5 N higher than the approximate value). The absence of an entry in Table I indicates that no cracks could be found in that experiment.

### 4. Discussion

The main features seen at indentations made at low loading rates (5 and 10 N s<sup>-1</sup>) and at the impact sites are in good agreement with previous work [2, 4, 7, 8, 12, 14–18]. Also, the true contact areas measured on coated glass slabs are in excellent agreement with the contact sizes predicted by Hertz theory

$$a^3 = \frac{3PR}{4E^*} \quad (1)$$

where  $a$  is the contact zone radius,  $P$  is the load,  $R$  is the radius of the indenter and

$$1/E^* = \left( \frac{1 - \nu^2}{E} + \frac{1 - \nu'^2}{E'} \right)$$

where  $\nu$  and  $E$  are Poisson's ratio and Young's modulus, respectively, with primes referring to the indenter material.

The type of damage encountered in the quasi-static experiments was as expected: ring, cone and lateral cracks and crushing at very high loads. The size of the ring crack (the largest one in the cases where more than one ring crack were present) was compared with the theoretical contact zone. Fig. 2 shows a plot of this relationship and a least squares fit to a linear function of the form  $y = C*x$  gives the ratio between measured ring crack radius and theoretical contact zone as 1.29. This is in good agreement with Chaudhri and Yoffe [4] and Johnson *et al.* [2]. The three data points clearly above the others in Fig. 2 have been examined carefully but no factor separating them as unique has been identified.

In order to make a more quantitative analysis, the fracture types can be ordered according to increasing maximum load,  $P_m$ . It should be noted here that the cracks are initiated at loads lower than  $P_m$ . This can account for some of the scatter in the recorded data. First we consider the low loading rate indentations ( $5$  and  $10 \text{ N s}^{-1}$ ). The first damage encountered is ring cracks induced at  $P_m = 200 \text{ N}$ . At  $P_m = 400\text{--}500 \text{ N}$ , one cone crack growing from a ring crack is added. At these loads there is usually more than one ring crack present. Next to occur at  $P_m = 500\text{--}1000 \text{ N}$  are lateral cracks extending almost parallel to the surface. Lateral cracks have, in some cases, led to material removal by chipping from the surface surrounding the indentation. At maximum loads between  $500$  and  $1000 \text{ N}$  lateral cracks can be seen in some indentations while at maximum loads above  $1000 \text{ N}$  these cracks are present in almost all cases. Also, in a few cases with maximum loads above  $800 \text{ N}$ , radial cracks are formed. At very high loads,  $P_m > 2500 \text{ N}$ , the material right below the indenter has been crushed. This corresponds to a mean pressure of several GPa below the indenting sphere, which probably exceeds the compressive strength of the glass. For example, Lankford [20] has reported compressive strengths of

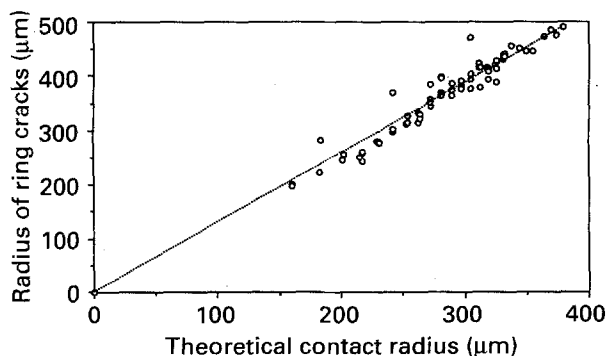


Figure 2 The relationship between (O) the measured radius of the largest ring crack and the calculated contact radius. (---) Least squares fit.

a glass-ceramic to be up to  $3.5 \text{ GPa}$  for dynamic loading conditions and  $2.8 \text{ GPa}$  for quasi-static conditions and ordinary glass should not exceed these figures.

When the loading rate is raised to  $100 \text{ N s}^{-1}$  or higher, some new and unexpected features in the cracking behaviour are encountered. At these loading rates no damage can be detected by optical microscopy on the glass until the maximum load is  $500 \text{ N}$  while at the lower loading rates cracks were always formed when the maximum load was  $200 \text{ N}$  or above. Nonetheless, the size of the damage is only dependent on the maximum load. This behaviour is unexpected because even at  $500 \text{ N s}^{-1}$  the experiment should be quasi-static. One possible explanation of this could be the moving boundary between high tensile stress (outside the contact zone) and compressive stress (inside the contact zone). This boundary "sweeps" outwards as the indenter is pressed into the glass plate. The very steep stress gradient at the boundary creates a fast transition from tension to compression during loading and the reverse during unloading. As the loading rate is raised the boundary moves faster and existing flaws will be subjected to the high tensile stress for a shorter time than at lower loading rates. If the flaws have some incubation time to reach a critical size this could result in the observed behaviour.

Another change when making the quasi-static indentations at high loading rates is that the ring cracks occupy a narrower zone although the size of the largest ring crack only depends on the maximum load, see Fig. 3. This means that the inner ring crack is larger than at lower loading rates, which would also be explained by the proposed theory above. The crack formation sequence according to increasing load remains the same as described for the lower loading rates with the exception that no ring cracks can be seen without an accompanying cone crack.

The size of the cone cracks is also dependent on the loading rate. At  $100$  and  $200 \text{ N s}^{-1}$  the cone cracks are much smaller than at the lower loading rates for the same maximum load. However, at  $500 \text{ N s}^{-1}$  the cone cracks are larger than at the low loading rates ( $\leq 10 \text{ N s}^{-1}$ ). This behaviour is unexpected, but the experiment has been repeated on different glass pieces with the same results. At present, no explanation of this behaviour can be given.

It is also notable that Hertz predicted that his solution was only applicable at low loads, that is when the ratio of contact zone radius to indenter radius is less than  $0.1$  ( $a/R < 0.1$ ). This corresponds to approximately  $P = 170 \text{ N}$  for the present system ( $3 \text{ mm}$  steel spheres on soda-lime glass). In this work all cases where cracks are encountered are above this limit. However, very good agreement is found between our experimentally measured contact zones and the ones predicted by Hertz theory. Further, from theoretical calculations by Yoffe [21], it is found that indenting a material with  $\nu = 0.25$  with a rigid indenter is in good agreement with Hertz theory up to  $a/R \approx 0.5$  with maximum numerical correction to the calculated  $a^3$  of  $2\%$ . In the present work the maximum contact radius is  $a/R \approx 0.3$ .

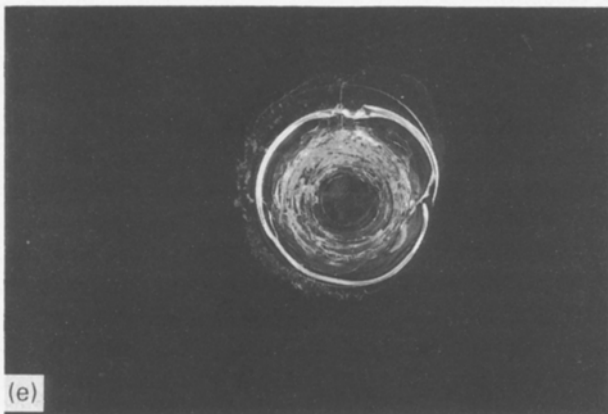
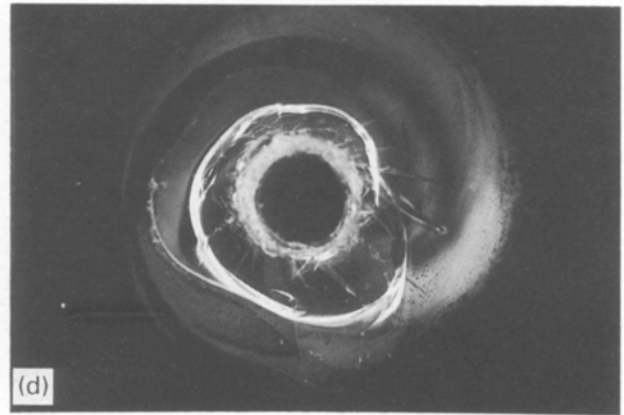
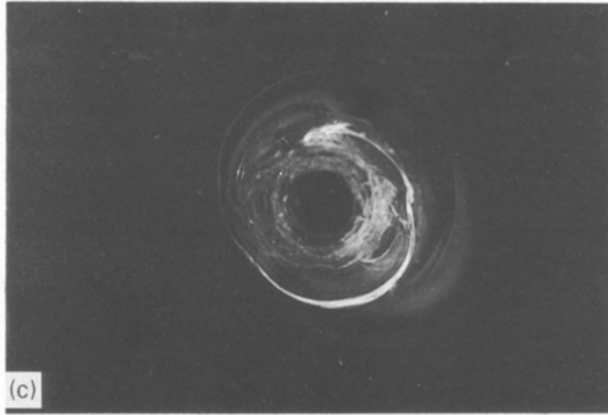
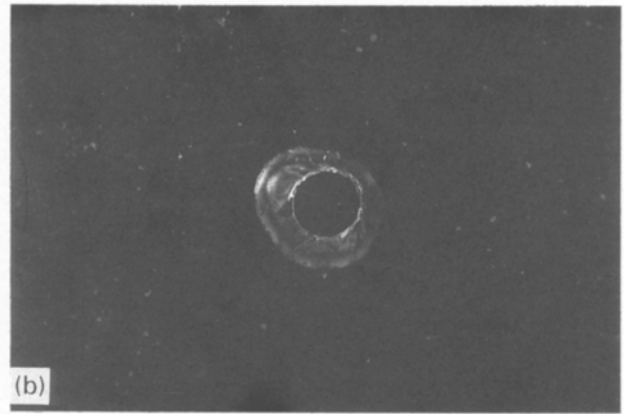
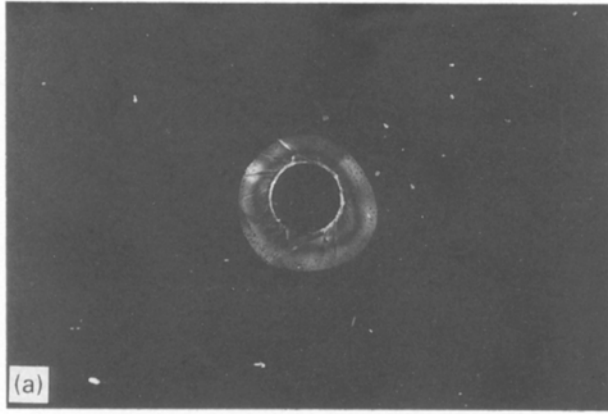


Figure 3 Indentations on glass with a 3 mm diameter hardened steel sphere at different maximum loads,  $P_m$  (N), and different loading rates,  $\dot{P}$  ( $\text{N s}^{-1}$ ). All photos have the same magnification. (a)  $P = 500$  N,  $\dot{P} = 5$   $\text{N s}^{-1}$ . Radius of the largest ring crack  $r = 258$   $\mu\text{m}$ . (b)  $P = 500$  N,  $\dot{P} = 500$   $\text{N s}^{-1}$ . Radius of the largest ring crack  $r = 249$   $\mu\text{m}$ . (c)  $P = 1800$  N,  $\dot{P} = 5$   $\text{N s}^{-1}$ . Radius of the largest ring crack  $r = 440$   $\mu\text{m}$ . (d)  $P = 1800$  N,  $\dot{P} = 500$   $\text{N s}^{-1}$ . Radius of the largest ring crack  $r = 430$   $\mu\text{m}$ ; (e)  $P = 1800$  N,  $\dot{P} = 100$   $\text{N s}^{-1}$ . Radius of the largest ring crack  $r = 435$   $\mu\text{m}$ .

In order to compare impacts with quasi-static experiments, a rough estimate of the mean loading rate encountered in an impact was made. Assuming that the maximum delivered load is of the order of a few thousand Newtons and the loading part of the cycle lasts a few microseconds, see Knight *et al.* [7] and Chaudhri [17], the mean loading rate will be of the order of  $0.1\text{--}1$   $\text{GN s}^{-1}$ , which is several orders of magnitude higher than the quasi-static tests. When the quasi-static indentations are compared with the impacts some similarities are apparent. The impacts made at low velocities have similar damage morphology to that of the quasi-static indentations made at high loading rates. If it is assumed, as a first approximation, that similar damage sizes should correspond to similar maximum load, comparison between quasi-static indentations and impacts can be made, as long as the damage encountered in the two cases is sim-

ilar. This comparison shows that impact velocity  $v = 30.9$   $\text{m s}^{-1}$  (ring crack radius  $r = 359$   $\mu\text{m}$ ) should correspond to maximum load  $P_m = 1000$  N. Similarly, impact velocity  $v = 44.6$   $\text{m s}^{-1}$  ( $r = 430$   $\mu\text{m}$ ) correspond to  $P_m \approx 1800$  N. This can be compared to the loads obtained from the equation used by Knight *et al.* [7] and Wiederhorn and Lawn [8]

$$P_m = \left[ \left( \frac{125\pi^3}{48} \right)^{1/5} \left( \frac{E}{k} \right)^{2/5} \rho^{3/5} R^2 \right] v^{6/5} \quad (2)$$

where

$$k = \left( \frac{9}{16} \right) \left[ (1 - v^2) + (1 - v'^2) \frac{E}{E'} \right]$$

(primes refer to indenter material) and  $\rho$  is the density of the impacting sphere. Using this equation for the two cases above gives  $P_m(v = 30.9$   $\text{m s}^{-1}) \approx 2800$  N and  $P_m(v = 44.6$   $\text{m s}^{-1}) \approx 4300$  N. The agreement between the two methods is not very good. There are some factors that can explain this. First, the estimate based on similar-sized damage can be too rough due to experimental scatter in the data. Second, Equation

2 is derived from static and fully elastic conditions and may not be fully accurate when cracking occurs in the material. Third, the material properties might be different for dynamic loading conditions compared to the quasi-static conditions where they are determined. The last point has been investigated by Lankford [20] where the compressive strength of several ceramics can be seen to increase with increasing confining pressure and strain rate.

Because of the uncertainty in maximum load delivered to the target plate, it is not possible to compare the experimentally determined crack sizes to theoretically calculated contact zones with any accuracy. It should also be remembered that the maximum load and loading rate are independently variable only in the quasi-static case while in the impact case both maximum load and loading rate depend on impact velocity.

At higher velocity impacts the damage begins to change from that encountered in quasi-static indentations. The differences are that the impacted glass pieces show radial cracks in almost all cases above a certain impact velocity ( $v \geq 35 \text{ m s}^{-1}$ ) and at still higher impact velocities ( $v \geq 45 \text{ m s}^{-1}$ ) the central area below the impacting sphere is crushed. Crushing is believed to be damage caused by compressive stresses while cracking is tensile stress damage, because the damaged zones coincide well with the quasi-static stress fields, as calculated by Zeng *et al.* [1]. Also, the central area is almost undamaged up to velocities where it is crushed.

As the impact velocity is raised above  $100 \text{ m s}^{-1}$ , the damaged surface zone reaches an approximately constant size, 12–15 mm in diameter. Instead of growing outwards the damage will penetrate deeper into the glass. Also the damage pattern will be more complex with a large number of radial and other cracks, especially right outside the crushed zone. The largest crack is always a lateral crack.

This confirms that the compressive strength of the material is an important material property to describe the resistance against impact-induced damage. When the projectile is much smaller than the target, it is the compressive strength of the confined material that is important, because the impact site is then supported by the surrounding material, see discussion by Shockey *et al.* [22]. When impacted by a heavier (larger) projectile, another important parameter is the ability to withstand large tensile stresses at the opposite side from the impact, due to bending of the plate [23]. This implies that a material with high compressive strength on the impact side and some ductility on the back side would be a good material to defeat impacts.

## 5. Conclusions

It is shown that Hertz theory for static, elastic contacts can be used to calculate the size of the contact zone as long as the damage induced in the target plate is only simple cracking without crushing. By comparing the damage morphologies of different maximum loads to the calculated stress fields it is concluded that cracking

is caused by tensile stresses while crushing is caused by compressive stresses. Therefore, it is reasonable that Hertz theory should break down when the highly non-elastic crushing occurs. With this in mind it can be said that cracking is to some extent "more elastic" damage than crushing. It should also be noted that, *in this case* (a steel sphere indenting a glass plate), Hertz theory can be used for  $a/R$  values larger than predicted in the original work. A new feature, previously not reported, is the loading-rate dependence of the damage. It is plausible that a transition from quasi-static to dynamic damage behaviour exists as the loading rate is increased but it was not expected to be seen at these, relatively low loading rates of just a few hundred Newtons per second. A rough estimate of the loading rate encountered in impact tests like these give a mean loading rate of the order of  $0.1\text{--}1 \text{ GN s}^{-1}$ .

Hertz theory can thus be used for low-velocity impacts up to the point where crushing occurs. As the impact velocity increases the material response deviates from the ideal quasi-static Hertzian behaviour to involve dynamic effects.

## Acknowledgements

This work is performed in cooperation with the Department of Solid Mechanics at the Royal Institute of Technology within a project sponsored by HB Utveckling AB.

## References

1. K. ZENG, K. BREDER and D. ROWCLIFFE, *Acta Metall. Mater.* **40** (1992) 2595.
2. K. L. JOHNSON, J. J. O'CONNOR and A. C. WOODWARD, *Proc. R. Soc. Lond. A* **334** (1973) 95.
3. P. S. FOLLANSBEE and G. B. SINCLAIR, *Int. J. Solids Struct.* **20** (1984) 81.
4. M. M. CHAUDHRI and E. H. YOFFE, *Philos. Mag. A* **44** (1981) 667.
5. F. C. FRANK and B. R. LAWN, *Proc. R. Soc. Lond. A* **299** (1967) 291.
6. K. L. JOHNSON, *Proc. Inst. Mech. Eng.* **196** (1982) 363.
7. C. G. KNIGHT, M. V. SWAIN and M. M. CHAUDHRI, *J. Mater. Sci.* **12** (1977) 1573.
8. S. M. WIEDERHORN and B. R. LAWN, *J. Am. Ceram. Soc.* **60** (1977) 451.
9. A. G. EVANS and T. R. WILSHAW, *Acta Metall.* **24** (1976) 939.
10. R. F. COOK and G. M. PHARR, *J. Am. Ceram. Soc.* **73** (1990) 787.
11. D. J. ROWCLIFFE, in "Erosion of Ceramic Materials" edited by J. E. Ritter (Trans Tech Publications, Zürich, 1992) p. 1.
12. K. ZENG, K. BREDER and D. ROWCLIFFE, *Acta Metall. Mater.* **40** (1992) 2601.
13. K. ZENG, K. BREDER, D. ROWCLIFFE and C. HERRSTRÖM, *J. Mater. Sci.* **27** (1992) 3789.
14. M. M. CHAUDHRI and C. R. KURKJIAN, *J. Am. Ceram. Soc.* **69** (1986) 404.
15. A. G. EVANS, M. E. GULDEN and M. ROSENBLATT, *Proc. R. Soc. Lond. A* **361** (1978) 343.
16. A. G. EVANS and T. R. WILSHAW, *J. Mater. Sci.* **12** (1977) 97.
17. M. M. CHAUDHRI, in "Strength of Inorganic Glasses", edited by C. R. Kurkjian (Plenum Press, New York, 1985) pp. 87–113.
18. M. M. CHAUDHRI and M. A. PHILLIPS, *Philos. Mag. A* **62** (1990) 1.

19. J. PERSSON, D. ROWCLIFFE and K. BREDER, in "Proceedings of the 4th International Symposium on Ceramic Materials and Components for Engines", edited by R. Carlsson (Elsevier, Essex, 1992) p. 507.
20. J. LANKFORD, personal communications (1992).
21. E. H. YOFFE, *Philos. Mag. A* **50** (1984) 813.
22. D. A. SHOCKEY, A. H. MARCHAND, S. R. SKAGGS, G. E. CORT, M. W. BURKETT and R. PARKER, *Int. J. Impact Eng.* **9** (1990) 263.
23. M. L. WILKINS, R. L. LANDINGHAM and C. A. HONODEL, Tech. Rept. UCRL-50980, Lawrence Radiation Laboratory, Livermore, CA (1971).

*Received 3 September 1992  
and accepted 7 May 1993*